Journal of Molecular Structure 917 (2009) 133–141

Contents lists available at ScienceDirect

Journal of Molecular Structure

journal homepage: www.elsevier.com/locate/molstruc

Structures and properties of 1,7-disubstituted perylene tetracarboxylic diimides: The substitutional effect study based on density functional theory calculations

Baolong Liang, Yuexing Zhang, Yanfeng Wang, Wei Xu, Xiyou Li *

Department of Chemistry, Shandong University, 27 Shandananlu Street, Jinan 250100, China

ARTICLE INFO

Article history:
Received 5 May 2008
Received in revised form 7 July 2008
Accepted 9 July 2008
Available online 17 July 2008

Keywords:
DFT calculation
Substitutional effect
Perylene tetracarboxylic diimide
Electronic absorption spectra
IR spectra

ABSTRACT

Density functional theory (DFT) calculations were carried out to describe the molecular structures, molecular orbitals, atomic charges, UV–vis absorption and IR spectra of 1,7-disubstituted-perylene-3,4;9,10-tetracarboxylic diimide (1,7-disubstituted PDI) with different substituents, namely unsubstituted PDI (PDI-0), 1,7-dimethylthio PDI (S-a), 1,7-dithiophenyl PDI (S-b), 1,7-dimethoxy PDI (O-a), 1,7-diphenoxy PDI (O-b), 1,7-dimethylamino PDI (N-a), 1-methoxy-7-methylthio PDI (OS-a), 1-phenoxy-7-thiophenyl PDI (OS-b), and 1-methoxy-7-methylamino PDI (ON-a). Good consistency was found between the calculated results and experimental data. The substitutional effects of the side groups on both the structure twisting and the electronic absorption spectra depend mainly on the linking atoms rather than the side groups as a whole. The charge distribution, the ionization energy (IE) and electronic affinity (EA) are found to be varied significantly along with the change of the electron donating abilities of the side groups. The effects of the side groups on the vibration spectra of these compounds are also discussed based on both the simulated and experimental results. The present work, representing the first systemic DFT study on the PDI derivatives, sheds further light on clearly understanding structure and spectroscopic properties of PDI compounds.

1. Introduction

Perylene tetracarboxylic diimides (PDI) and their derivatives have attracted more and more attentions in the past decade due to not only their outstanding thermal and photochemical stabilities [1,2], but also their large application potential in organic optoelectronic or electronic devices [3–11], such as field effect transistors, solar cells [12–20], light-harvesting arrays [21–25], and light emitting diodes [25–30]. Furthermore, molecular modification of PDIs can be achieved easily by introducing different groups at imide nitrogens or the bay positions (1,6,7,12), which can in turn tune the physical properties or endow these compounds with liquid crystal properties, controllable nano- and mesoscopic supramolecular structures [31–46].

In recent years, along with the development of computer industry and calculation method, calculations and simulations on large molecular and even supramolecular systems at more accurate level become possible. Density functional theory (DFT) methods, at the B3LYP level, have proved suitable for the energy-minimized structure and property calculations for polycyclic aromatic compounds recently [47]. The ground state properties of a series of polycyclic aromatic compounds namely naphthalene, pyrene, benzopyrene, perylene, terrrylene, and their derivatives have been calculated using density functional theory at the B3LYP level [47–50]. At the same time, the efficiency of time-dependent density functional theory (TDDFT) on calculating electronic absorption spectra was also well demonstrated [51–53]. The properties of PDI molecules in vacuum [47,52–55] and the properties of some PDI derivatives on the surface of Si, Au and Ag [56,57] have been calculated using DFT method. More recently, the interaction of alkali azide with perylene derivatives are discussed using vibrational spectroscopy method [58,59]. The influence of substituents at the imide nitrogen atoms on the frontier orbital are reported by F. Pichierri et al. [54]. However, the detailed effects of various substituents at the bay positions on the properties of the PDI are still not clear. The systematically studies of a series of 1,7-substituted PDI derivatives with different substituents is necessary to illustrate the effects of substituents on the physical properties of PDI more amply.

In the present work, nine 1,7-disubstituted PDI compounds were calculated using DFT method at the B3LYP/6-31G(d) level. The effects of side groups at 1,7-positions with different electronic properties on the structure parameters, atomic charges, molecular orbitals, IR, and electronic absorption spectra of these PDI derivatives are systematically discussed. The IR and electronic absorption spectra are assigned and identified in detail by comparing with the experimental results.

* Corresponding author. Tel.: +86 531 8836 9877; fax: +86 531 8856 4464.
E-mail address: xiyouli@sdu.edu.cn (X. Li).

0022-2860/$ - see front matter © 2008 Elsevier B.V. All rights reserved.
doi:10.1016/j.molstruc.2008.07.005

2. Experiments

PDI and their derivatives, namely 1,7-didodecylthio PDI, 1,7-dithiophenyl PDI, 1,7-didodecyloxy PDI, 1,7-diphenoxy PDI, 1-dodecyloxy-7-dodecylthio PDI, 1-phenoxy-7-thiophenyl PDI, 1,7-didodecylamino PDI, and 1-dodecylamino-7-dodecyloxy PDI, were prepared and purified according to the literature [42,46,60] in our lab. IR spectrum was recorded from KBr disks using a VERTEX-70 spectrometer in the range of 4000–400 cm^{-1} with a resolution of 2 cm^{-1}. Electronic absorption spectra were recorded at room temperature on a Hitachi U-4100 spectrophotometer in chloroform.

2.1. Computational details

The structures of these nine PDIs are simplified during the DFT calculation as shown in Fig. 1. The hybrid density function B3LYP (Becke–Lee–Young–Parr composite of exchange-correction functional) method [48,49,61,62] and the standard 6-31G(d) basis set [55,64] were used for both structure optimization and the property calculations, which has been proved to be more accurate in simulating vibrational spectra compared with the Hartree–Fock method [47]. On the basis of the optimized structures, IR frequency calculations were carried out using the same method and basis set as the optimization step. No imaginary frequency is predicted, indicating that the optimized structures are true energy-minimums. DFT calculations is found to overestimate the vibrational frequencies often compared with the experimental data due to the neglect of anharmonicity effect and the incomplete incorporation of electron correction in the theoretical treatment [59], which, however, is uniform for a range of frequencies and thus can be corrected with generic frequency scaling factors. As a result, the calculated frequencies with 6-31G(d) basis set in this work are scaled down using a scaling factor of 0.9613 [62,63]. Based on the energy-minimized structure generated in the last step, charge population calculations were carried out with a full natural bond orbital analysis (NBO) population method [64] and the molecular orbital distribution are discussed according to the NBO results. Electronic absorption calculations were performed using TDDFT method at B3LYP/6-31G(d) level, which allowed us to provide a detailed assignment of the excited-states and vertical excitation energy involved in the absorption process. With the help of the SWIZARD software [65], the calculated electronic absorption data of all these compounds were simulated to sequential absorption spectrum, which can be compared directly with the experimental absorption spectrum. Ionization energy (IE) and electronic affinities (EA) were also calculated through the energy differences between anions or cations and the neutral molecule. All the calculations were performed using the Gaussian 03 program [66] in the IBM P690 system at the Shandong Province High Performance Computing Centre.

3. Results and discussion

3.1. Minimized molecular structures

The optimized structure of unsubstituted PDI-0 is C_{2v} symmetry while compounds N-a, O-a, O-b, S-a, and S-b are C_2 symmetry. But compounds OS-a, OS-b, and ON-a, which are substituted with different groups at 1,7 positions are C_1 symmetry. Table 1 compares our calculated structure parameters of PDI-0 with X-ray crystallography data. As can been seen from Table 1, the calculated results agrees very well with the experimental ones. The largest difference on bond length presented by C_{13}–C_{14} is only 0.02 Å while the largest difference on tilting angle is as small as 1°, which indicates that our calculation method is reliable for simulating PDI compounds.

Table 2 summarized the bond length of PDI core and twist angles of the two naphthalene rings for PDI-0, O-a, O-b, S-a, S-b, OS-a, OS-b, N-a, and ON-a. It can be seen that, PDI-0 has a planar structure with the twisting angle between the two naphthalene rings close to 0°. However, when substituents are introduced at the bay positions, the planar structure is disturbed with a significant twisting angle between the naphthalene rings due to the steric hindrance [2]. The twisting angles between the two naphthalene rings in the substituted PDIs varied in the range of 13.7–21.7° depending on the substituents at the 1,7-positions. The linking atoms between the substituents and the perylene ring play a dominating role on determine the twisting angles between the naphthalene rings as revealed by the results in Table 2. For example, the twisting angles between the naphthalene rings of O-a is 13.8°, which is significantly smaller than that of S-a (21.1°) due to the smaller atomic radii of O than S [67]. Same results can also be drawn from the comparison of the twisting angles between S-b and O-b (21.7 vs. 13.7°) as well as the different twisting angles

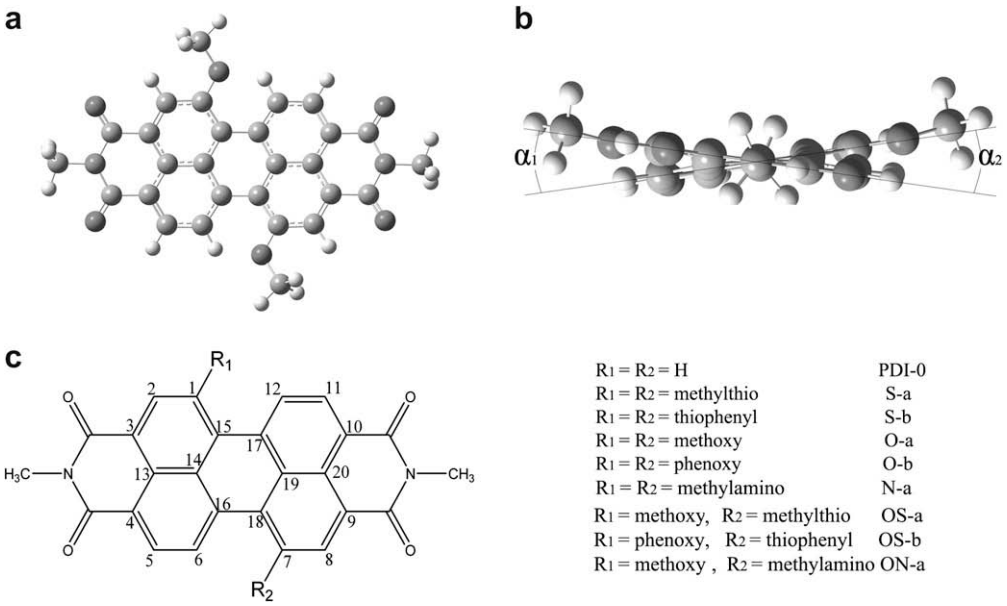

Fig. 1. Top view (a) and side view (b) of the minimized structure of S-a and the molecular structure of 1,7-disubstituted PDIs (c).

Table 1
The calculated and experimental structure parameters of PDI-0 (Å for bond length and degree for bond angle)

Parameter[a]	C_1–C_2	C_2–C_3	C_3–C_{13}	C_{13}–C_{14}	C_{13}–C_4	C_4–C_5	C_5–C_6	C_6–C_{16}	C_{16}–C_{18}	C_{14}–C_{15}	C_{14}–C_{16}	α
Cal.	1.399	1.384	1.416	1.429	1.416	1.384	1.399	1.396	1.471	1.431	1.431	−0.008
Exp.[b]	1.396	1.365	1.422	1.409	1.422	1.365	1.396	1.383	1.457	1.423	1.423	−1.188

[a] See Fig. 1 for atomic label.
[b] Exp. data taken from Ref. [69].

Table 2
The calculated bond lengths (Å) and twisting angles α (°) of 1,7-disubstituted PDIs

Parameter[a]	PDI-0	S-a	S-b	OS-b	O-b	OS-a	O-a	ON-a	N-a
C_1–C_2	1.399	1.410	1.411	1.405	1.404	1.405	1.404	1.403	1.415
C_2–C_3	1.384	1.379	1.378	1.378	1.377	1.380	1.379	1.381	1.377
C_3–C_{13}	1.416	1.412	1.414	1.414	1.415	1.410	1.411	1.410	1.413
C_{13}–C_{14}	1.429	1.425	1.425	1.427	1.430	1.429	1.431	1.430	1.427
C_{13}–C_4	1.416	1.415	1.414	1.416	1.415	1.416	1.416	1.417	1.414
C_4–C_5	1.384	1.383	1.384	1.383	1.382	1.382	1.382	1.383	1.385
C_5–C_6	1.399	1.400	1.400	1.400	1.398	1.400	1.398	1.398	1.398
C_6–C_{16}	1.396	1.399	1.399	1.399	1.402	1.398	1.402	1.404	1.405
C_{16}–C_{18}	1.471	1.465	1.465	1.464	1.470	1.464	1.469	1.464	1.465
C_{18}–C_7	1.396	1.419	1.415	1.415	1.411	1.419	1.419	1.426	1.426
C_7–C_8	1.399	1.410	1.411	1.411	1.404	1.409	1.404	1.416	1.415
C_8–C_9	1.384	1.379	1.378	1.377	1.377	1.378	1.379	1.376	1.377
C_9–C_{20}	1.416	1.412	1.414	1.415	1.415	1.413	1.411	1.415	1.413
C_{20}–C_{19}	1.429	1.425	1.425	1.427	1.415	1.427	1.431	1.428	1.427
C_{20}–C_{10}	1.416	1.415	1.414	1.413	1.415	1.414	1.416	1.412	1.414
C_{10}–C_{11}	1.384	1.383	1.384	1.384	1.382	1.383	1.382	1.384	1.385
C_{11}–C_{12}	1.399	1.400	1.400	1.398	1.398	1.398	1.398	1.397	1.398
C_{12}–C_{17}	1.040	1.399	1.399	1.402	1.402	1.402	1.402	1.403	1.405
C_{17}–C_{15}	1.471	1.465	1.465	1.469	1.470	1.469	1.469	1.469	1.465
C_1–C_{15}	1.396	1.419	1.415	1.410	1.411	1.418	1.419	1.419	1.426
C_{14}–C_{15}	1.431	1.433	1.435	1.434	1.436	1.430	1.433	1.432	1.430
C_{14}–C_{16}	1.431	1.436	1.435	1.434	1.437	1.436	1.440	1.439	1.438
C_{19}–C_{17}	1.431	1.436	1.435	1.437	1.437	1.439	1.440	1.438	1.438
C_{19}–C_{18}	1.431	1.433	1.435	1.436	1.436	1.435	1.433	1.431	1.430
α_1	0.003	21.416	21.660	14.857	13.685	14.685	13.802	15.033	21.073
α_2	0.003	21.416	21.660	21.170	13.685	21.104	13.802	20.655	21.073

[a] See Fig. 1 for atomic labels.

between the two sides with different substituents in both OS-a and OS-b (21.2° and 21.1° vs. 14.9° and 14.7°, respectively). It is interesting that the difference of the twisting angles between S-a and S-b are neglectable (21.7 vs. 21.1°), indicating that the groups linked at S do not contribute to the twisting angles a lot. This result is also supported by the similar twisting angles between O-a and O-b. The atomic radius of nitrogen is similar with that of oxygen and much smaller than that of sulfur [68]. However, the twisting angle of N-a (21.1°) is much larger than that of O-a and close to that of S-a. This is because two atoms (H and C) were connected directly to nitrogen atom while only one atom was connected with sulfur or oxygen atoms. The former brings large repulsions between the hydrogen atoms at 6 and/ or 12 positions of perylene ring with the substituents at 1,7 positions.

In addition to the twisting angle, the introduction of the substituents also induces the change of bond length for the perylene rings. As listed in Table 2, the bonds which close to the 1, 7 positions of the perylene ring, including C_1–C_2, C_1–C_{15}, C_2–C_3, C_3–C_{13}, C_6–C_{16}, C_7–C_8, C_{18}–C_7, C_8–C_9, C_9–C_{20}, and C_{12}–C_{17} are all elongated a little bit when the side groups are introduced at 1,7 positions. The bonds C_1–C_{15} and C_{18}–C_7 were mostly impacted probably because of their adjacency with the substituents. The bond length of C_1–C_{15} and C_{18}–C_7 in PDI-0 is 1.396 Å, which increased to 1.419 Å in O-a and S-a and 1.426 in N-a. This result suggested that the radius of the linking atom do not affected the bond length of C_1–C_{15} and C_{18}–C_7 obviously. The extra large bond length of C_1–C_{15} and C_{18}–C_7 in N-a can be ascribed to either the large steric hindrance introduced by the two atoms connected at nitrogen atoms or the participation of the lone pair of nitrogen atom to the conjugation of perylene ring. The bond length of C_{18}–C_7 and C_1–C_{15} in S-b is 1.415 Å, which is larger than that of O-b, suggesting that thiophenyl groups present stronger effect than phenoxy groups on the bond length of C_{18}–C_7 and C_1–C_{15}. This is also supported by the fact that the C_{18}–C_7 bond in OS-b is longer than C_1–C_{15} bond, 1.415 vs. 1.410 Å. The bond length of C_{18}–C_7 and C_1–C_{15} in S-b is larger than that in S-a while the bond length of the same bonds in O-b is smaller than those in O-a. This controversial result indicates that the effects of methoxy and phenoxy groups on the bond length of C_{18}–C_7 and C_1–C_{15} can not be simply attributed to the steric hindrance, other effects, such as electronic effect, need to be taken into account.

The bonds C_1–C_2 and C_7–C_8 are also strongly affected by the substituents. The largest bond length of C_1–C_2 and C_7–C_8 was presented by compound N-a, which is significantly larger than that in compound O-a and S-a. This can be attributed to both the larger steric hindrance as well as the electronic effects as mentioned above. Different from bonds C_{18}–C_7 and C_1–C_{15}, bonds C_1–C_2 and C_7–C_8 were significantly affected by the radius of the linking atoms. For example, length of bonds C_1–C_2 and C_7–C_8 in O-a is 1.404 Å, which is smaller than that of S-a (1.411 Å). Similar results can be found from the comparison of the bond length of C_1–C_2 and C_7–C_8 in compound O-b and S-b.

3.2. Molecular orbitals

The energies of the molecular orbitals from HOMO-5 to LUMO + 5 and energy gaps between LUMO and HOMO are shown in Fig. 2. It should be mentioned that the absolute values of the

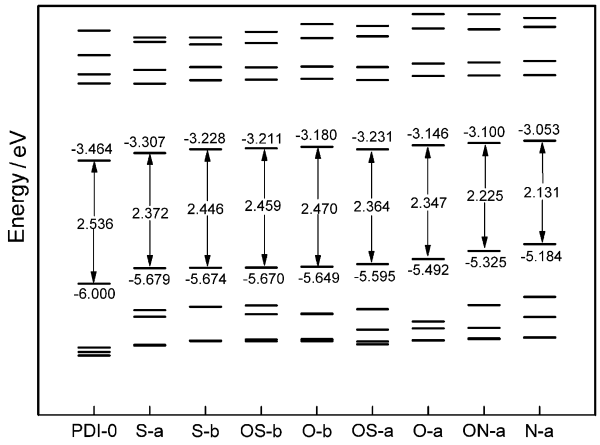

Fig. 2. The calculated energy levels from HOMO-5 to LUMO + 5 and the energy gaps between LUMO and HOMO of the 1,7-disubstituted PDIs.

molecular orbital energies have no practical meanings due to the fact that DFT method significantly underestimates orbital gaps because of the incorrect standard exchange function. However, the calculated results are still useful and reasonable in comparing molecules with similar structures if the same method and basis set are used. As shown in Fig. 2, the HOMO and LUMO levels of PDI-0 are −0.600 and −3.464 eV, respectively, with the HOMO–LUMO energy gap of 2.536 eV. When electron-donating groups are introduced to the 1,7-position of the perylene ring, the energy levels of both HOMO and LUMO are increased a little bit but the increase of HOMO energy is larger than that of LUMO. As a consequence, the HOMO–LUMO energy gap decreases along with the introduction of electron-donating substituents.

Furthermore, the increase in the energy level of the frontier orbital is found to depend on the properties of the substituents at 1,7-positions of PDI ring too. As shown in Fig. 2, both the HOMO and LUMO energies increase in the order of S-a < O-a < N-a, with the HOMO orbital energy level increased from −5.679 eV of S-a, through −5.492 eV of O-a, to −5.184 eV of N-a, while the LUMO energy level increase from −3.307 eV for S-a, through −3.146 eV for O-a, to −3.053 eV of N-a. As a result, the HOMO–LUMO energy gap decreases in the same order, from 2.372 eV for S-a, through 2.347 eV for O-a, to 2.131 eV for N-a. As expected, the HOMO and LUMO energy of OS-a and ON-a is found to lie between S-a and O-a and between O-a and N-a, respectively.

N-a has the highest HOMO and LUMO energy levels and smallest HOMO–LUMO energy gap among these series compounds, indicating the largest influence of methylamino group on the molecular orbital of PDIs. The effects of methylamino groups can not be attributed simply to the steric hindrance of methylamino groups, the electronic effects of the lone pair on the nitrogen atom must be taken into account. This is in line with the simulated electronic absorption spectra for these series compounds as detailed below.

The HOMO and LUMO energy of phenyl-including PDIs increase in the order of S-b < OS-b < O-b, which is same as that of methyl containing PDIs (O-a, S-a and N-a). However, the HOMO–LUMO Energy gap of phenyl-including PDIs increases following the same order: S-b < OS-b < O-b, which is contrary to the observation of methyl containing PDIs as mentioned above. The probable reason is the electronic interactions between the phenyl group and the linking atom has reduced the contribution of linking atom to the HOMO and LUMO while the methyl group does not electronically interact with the linking atom significantly.

To explain the effects of the side groups on the frontier molecular orbital energy level and the HOMO/LUMO energy gap more directly, we have calculated the contributions of the side groups to the HOMO and LUMO in these series of compounds, and the results are summarized in Table 3. It can be found that the contribution of side groups to HOMO is significantly larger than that to LUMO, therefore the increase of the energy level of HOMO due to the introduction of side groups at 1, 7 positions are larger than that of LUMO. However, the detailed analysis revealed that the contribution magnitude of the side groups to the HOMO or LUMO do not corresponding well with the energy levels of the HOMO and LUMO. This indicates that beside the electronic interactions, other effects, such as steric hindrance, play a role in determining the HOMO and LUMO energy levels as well.

Table 3
Contribution of the side groups to HOMO and LUMO of 1,7-disubstituted PDIs

	S-a	S-b	OS-b	O-b	OS-a	O-a	ON-a	N-a
HOMO	0.282	0.266	0.202	0.130	0.201	0.124	0.215	0.272
LUMO	0.109	0.079	0.063	0.096	0.056	0.047	0.060	0.069
LUMO/HOMO	0.387	0.297	0.312	0.738	0.279	0.379	0.279	0.254

It is worth noting that most of the contribution of side groups at 1,7 positions to the HOMO orbital comes from the linking atoms of substitutents according to our calculated NBO orbital distributions. However, this contribution is affected by the methyl or phenyl groups connected. The contribution proportion of sulfur atoms to the orbital segment on substituents of the HOMO is 0.655 in S-a while the proportion decreased to 0.612 in S-b. Similar effects have also been found in the comparison of the contribution of oxygen to the HOMO in compound O-a (0.598) and O-b (0.464). These results suggest that the phenyl groups reduce the contribution of linking atoms to the HOMO of PDIs relative to the methyl groups.

3.3. Atomic charge

The charge population was calculated at B3LYP/6-31G(d) level using a full natural bond orbital analysis method based on the energy-minimized structure optimized at the same level and the results were organized in Table 4. For PDI-0, the charge distributed on C_2 and C_8 are both −0.158 e, while that on C_1, C_6, and C_7 are −0.200 e. The charges on C_{12}, C_{15} and C_{18} are very small, −0.009 e. When electron-rich groups are introduced to the 1,7 positions of the PDI core, the charge distributed on perylene ring is strongly impacted. The negative charge distributed on C_2, C_8, C_{15} and C_{18} all decrease with different degrees. The most remarkable change of the charge distribution happened on C_1 and C_7. In S-a, the negative charge distributed at C_1 and C_7 is −0.167 e, which decreased for −0.033 e relative to that in PDI-0. But in O-a and N-a, the value changed from negative to positive, resulting in 0.352, and 0.206 e, respectively for C_1 and C_7, indicating the much stronger electronic attractive abilities of oxygen and nitrogen atoms relative to sulfur atoms. This is also supported by the fact that the charge on C_1 in compound O-b is 0.337 e while that in compound S-b is −0.164 e. It is worth noting that the charge on C_1 directly reflects the polarities of C_1–O, C_1–N and C_1–S bonds, which determined dominantly by the electronic affinities of the O, N, and S atoms. The charge distributed on C_{15} and C_{18} was also significantly increased due to the introduction of side groups at 1,7 positions. The charge on C_{15} and C_{18} are almost zero in PDI-0, −0.009 e, but in the substituted PDIs, the charge is increased significantly. The increase of the charge densities on these two atoms is resulted from the conjugation of linking atoms with the perylene ring and reflects directly the electron donating abilities of the side groups. The largest charge density increase presented by N-a indicates that methylamino group is the most powerful electron donating group comparing with methoxy or methylthio groups.

Table 4
Charge population (e) of 1,7-disubstituted PDIs calculated at the B3LYP/6-31G(d) level using NBO method

Atomic label[a]	PDI-0	S-a	S-b	OS-b	O-b	OS-a	O-a	ON-a	N-a
1	−0.1997	−0.1672	−0.1639	0.3376	0.3369	0.3541	0.3519	0.3466	0.2057
2	−0.1581	−0.1836	−0.1718	−0.2138	−0.2140	−0.2426	−0.2425	−0.2401	−0.2113
3	−0.1222	−0.1131	−0.1165	−0.1121	−0.1119	−0.1054	−0.1063	−0.1121	−0.1085
4	−0.1221	−0.1243	−0.1236	−0.1233	−0.1256	−0.1230	−0.1271	−0.1344	−0.1297
5	−0.1588	−0.1603	−0.1613	−0.1614	−0.1643	−0.1621	−0.1656	−0.1620	−0.1694
6	−0.1995	−0.2095	−0.2086	−0.2080	−0.2010	−0.2089	−0.2022	−0.2534	−0.2474
7	−0.1995	−0.1672	−0.1639	−0.1648	0.3369	−0.1691	0.3519	0.2110	0.2057
8	−0.1588	−0.1836	−0.1718	−0.1717	−0.2140	−0.1841	−0.2425	−0.2129	−0.2113
9	−0.1221	−0.1131	−0.1165	−0.1167	−0.1119	−0.1142	−0.1063	−0.1031	−0.1085
10	−0.1222	−0.1243	−0.1236	−0.1256	−0.1256	−0.1281	−0.1271	−0.1224	−0.1297
11	−0.1581	−0.1603	−0.1613	−0.1641	−0.1643	−0.1638	−0.1656	−0.1743	−0.1694
12	−0.1997	−0.2095	−0.2086	−0.2006	−0.2010	−0.2019	−0.2022	−0.1974	−0.2474
13	−0.0073	−0.0174	−0.0166	−0.0220	−0.0219	−0.0253	−0.0249	0.0022	−0.0283
14	−0.0149	−0.0012	−0.0022	−0.0012	−0.0023	−0.0001	−0.0016	−0.0037	0.0003
15	−0.0095	−0.0219	−0.0247	−0.0521	−0.0533	−0.0540	−0.0546	−0.0491	−0.0576
16	−0.0099	−0.0117	−0.0126	−0.0125	−0.0167	−0.0126	−0.0149	−0.0077	−0.0146
17	−0.0095	−0.0117	−0.0126	−0.0165	−0.0167	−0.0132	−0.0149	−0.0215	−0.0146
18	−0.0099	−0.0219	−0.0247	−0.0247	−0.0533	−0.0209	−0.0546	−0.0625	−0.0576
19	−0.0149	−0.0012	−0.0022	−0.0036	−0.0023	−0.0029	−0.0016	−0.0216	0.0003
20	−0.0073	−0.0174	−0.0166	−0.0165	−0.0219	−0.0172	−0.0249	−0.0317	−0.0283

[a] See Fig. 1 for atomic labels.

3.4. Absorption spectra

The calculations of electronic absorption spectra are carried out using time-dependent DFT method at the B3LYP/6-31G(d) level. On the basis of the calculated vertical excited energies and their corresponding oscillator strengths (Table 5), the continuous absorption spectra were simulated with the help of SWIZARD software with the width at half-height of 2500 cm^{-1}. The data of the simulated absorption spectra compared with that of the experimental absorption spectra for all the PDIs are summarized in Table 5. Fig. 3 compares the simulated and experimental recorded absorption spectra of S-a as representative. The spectra of other compounds are shown in supporting information. Good consistency between the simulated and experimental absorption spectra for most of the calculated PDIs is achieved, indicating the good efficiency of TDDFT method in calculating electronic absorption spectra of PDIs. However, it is worth noting that the maximum absorption wavelength of most compounds shows blue shift ranging from 4 to 63 nm relative to the corresponding experimental result. Compounds N-a and ON-a present the largest discrepancies between the simulated and experimental spectra in this series of compounds. But when the solvent effect is taken into account in calculating using IEF PCM method, the discrepancies for N-a and ON-a will both be reduced to less than 5 nm, suggesting that the solvents effect on the absorption spectra of these two compounds are extremely large. However, the first vertical excited energies of other compounds were seriously under estimated when the solvent effects are taken into account. The "inaccuracy" of TDDFT calculated electronic absorption spectra can be attributed to either the intrinsic shortcomings of this method which brings systematic error to some extent or the simplified molecular models used during the calculation and the solvent effects of chloroform during the experimental spectroscopy recording.

Moreover, the experimental absorption spectra of O-a and O-b present two peaks in the range of 450–550 nm while the simulated spectra give one peak only. This discrepancy might be the results of the avoidless very small amount of dimer due to the strong π–π interactions in solution, which causes blue shifted absorption peaks in this region [52].

Three or more absorption bands are observed in the simulated absorption spectra of these compounds. The maximum absorption band in the visible region, corresponding to the transition with the smallest excitation energy, is found always above 500 nm. Introducing of methylthio, methoxy or phenoxy groups at the bay positions of perylene ring induce significant red shift of this absorption peak. For example, compound PDI-0 show the absorption at 526 nm, which shift to 549 nm for O-a, 566 nm for S-a, and 612 nm for N-a. These absorption peaks at the longest wavelength are assigned to the electronic transition from HOMO to LUMO according to the calculation. The small peaks corresponding to the second smallest energy transition appear in the range of 300–450 nm, mainly due to the electronic transition from HOMO-1 or HOMO-2 to LUMO. Detailed assignments of other peaks are comparatively listed in Table 5.

The red-shift of the maximum absorption band in visible region due to the introducing of electron donating groups is affected by the side groups too. As can be seen in Fig. 4, the red shift of the maximum absorption peak of O-a, S-a, and N-a relative to PDI-0 increase following the order of O-a < S-a < N-a, which is somewhat different from the order of HOMO–LUMO energy gap (S-a < O-a < N-a) despite that these absorptions are mainly due to electronic transition from HOMO to LUMO according to the TDDFT calculation. The probable reason is the small contributions from the extra essential electronic transitions to the absorption which have shifted the peak wavelength of the maximum absorption in O-a or S-a. Same order reverse has also been observed between the shift of peak wavelength of the maximum absorption and the magnitude of HOMO–LUMO energy gaps of O-b and S-b. The peak wavelength of the maximum absorption in visible region of other compounds corresponds well with their HOMO–LUMO energy gaps.

In addition, the energy levels of both triplet states and singlet states of these series compounds were estimated by calculating the vertical excited energy of the transition from ground state to the first triplet states or first singlet state with TDDFT. The results are listed in Table 6. As expected the excited energy of triplet state is significantly smaller than that of the first singlet excited energy. The substitution at the bay positions reduces the energy of the first singlet state significantly compared with PDI-0 as shown by the calculated results. However, the effects of substitution on the energy levels of triplet states are more complicated. The methyl-substitution (CH_3O or CH_3S) reduced the triplet excited energy relative to PDI-0 with the order of N-a < O-a < S-a while the phenoxyl or thiophenyl groups increase the energy levels of triplet states. This result suggests that phenyl groups contributed to the triplet states efficiently. The energy of the first triplet excited energy increased

Table 5
The vertical excited energies, oscillatory strengths (f), experimental and calculated absorption wavelengths, and assignments of the electronic absorption spectra of 1,7-disubstituted PDIs

Compounds	Calculated			Experimental[a] (nm)	Assignment
	E (eV)	Wavelength (nm)	*f*		
PDI-0	2.4	508	0.6684	526	H-0 → L + 0(+75%)
	3. 8	328	0.0827	459	H-7 → L + 0(+80%) H-0 → L + 4(11%)
	5.7	218	0.6498	262	H-3 → L + 3(+51%)
S-a	2.2	566	0.4486	572	H-0 → L + 0(+77%)
	3.0	418	0.1974	430	H-2 → L + 0(+86%)
	4.4	280	0.1974	280	H-0 → L + 4(+45%) H-12 → L + 0(24%)
	5.4	229	0.8296		H-5 → L + 2(+56%)
S-b	2.3	552	0.5227	556	H-0 → L + 0(+77%)
	2.9	435	0.2117	442	H-1 → L + 0(+87%)
	4. 4	279	0.2192	282	H-0 → L + 5(+36%) H-16 → L + 0(34%)
	5.3	233	0.4382		H-6 → L + 2(+39%) H-8 → L + 2(+20%)
OS-b	2.3	541	0.5613		H-0 → L + 0(+76%)
	2.8	439	0.1209		H-1 → L + 0(+87%)
	4.5	275	0.2307		H-0 → L + 5(+45%)
	5.4	231	0.3181		H-9 → L + 2(+17%) H-2 → L + 7(13%)
O-b	2.3	529	0.6316	546	H-0 → L + 0(+76%)
	3.0	413	0.1616	404	H-1 → L + 0(+92%)
	3.9	323	0.0384		H-10 → L + 0(+86%)
	4.6	271	0.1458		H-0 → L + 4(+40%) H-2 → L + 2(+34%)
	5.4	229	0.3321		H-9 → L + 2(+32%)
OS-a	2.2	556	0.5142	568	H-0 → L + 0(+75%)
	2.8	429	0.0943	452	H-1 → L + 0(+88%)
	3.2	383	0.0532	408	H-2 → L + 0(+72%)
	4.5	276	0.1774	276	H-0 → L + 4(+41%)
	5.4	230	0.4677		H-5 → L + 2(+26%)
O-a	2.3	550	0.613	572	H-0 → L + 0(+74%)
	3.3	375	0.0652	394	H-2 → L + 0(+60%) H-4 → L + 0(+27%)
	3.9	322	0.0526		H-6 → L + 0(+90%)
	4.7	266	0.1134	274	H-1 → L + 2(+66%) H-5 → L + 1(15%)
	5.4	230	0.0724		H-10 → L + 1(+66%)
ON-a	2.1	588	0.4972	644	H → L(+73%)
	2.9	423	0.0728	448	H-1 → L + 0(+84%)
	3.3	382	0.0018	404	H → L + 2(+90%)
	4.5	279	0.0911	276	H-0 → L + 4(25%)
	5.6	223	0.0147		H-0 → L + 7(+28%) H-7 → L + 2(21%)
N-a	2.0	621	0.4541	684	H-0 → L + 0(+73%)
	3.2	386	0.1468	420	H-2 → L + 0(+84%) H-0 → L + 4(+8%)
	4.3	287	0.2154	286	H-1 → L + 2(+52%) H-0 → L + 4(24%)

[a] Exp. data taken from [42].

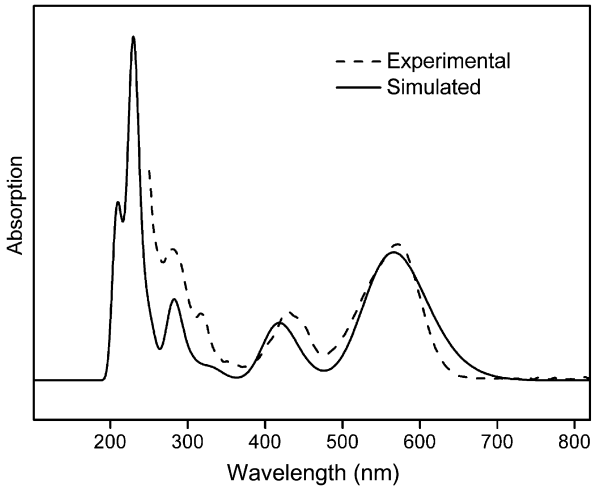

Fig. 3. Simulated (solid) and experimental (dash) electronic absorption spectra of S-a.

from 1.2636 eV of O-b, through 1.2762 eV of OS-b, to 1.2863 eV of S-b, indicating a larger impact of thiophenyl groups than that of phenoxyl groups on the energy of triplet excited states.

3.5. Infrared spectra

The simulated IR spectrum of PDI-0 is compared with the experimental spectrum in Fig. 5. As can be seen, the simulated spectrum corresponds well to the experimental one. A plot of the experimental peak positions (ν_{exp}) *vs* the calculated ones (ν_{cal}), Fig. 6, reveals the intuitional relationship of calculated and experimental data by fitting them to a linear function. The slope of line is 0.9545, which shows good consistency between the calculated and experimental data, indicating the good efficiency of the DFT method at the B3LYP/6-31G(d) level in calculating IR spectrum.

The simulated IR spectra of these compounds are shown in Fig. 7. The peak at 2970 cm^{-1} for unsubstituted PDI-0 is assigned as the symmetric NC–H stretching vibration of methyl group linked to the imide nitrogen while the peak at 3028 cm^{-1} is assigned as the asymmetric stretching vibration of the same bond. The peaks at 3093 and 3118 cm^{-1} are the symmetric and asymmetric stretching vibration of C–H at position 1, 2, 5, 6, 7, 8, 11 and 12 of perylene ring.

When methyl containing groups (CH_3O–, CH_3N– and CH_3S–) are introduced to the 1,7 positions of PDI, the peak at 2970 cm^{-1}, corresponding to the symmetric stretching of C–H of the methyl group attached at imide nitrogen, are intensified by the side groups fol-

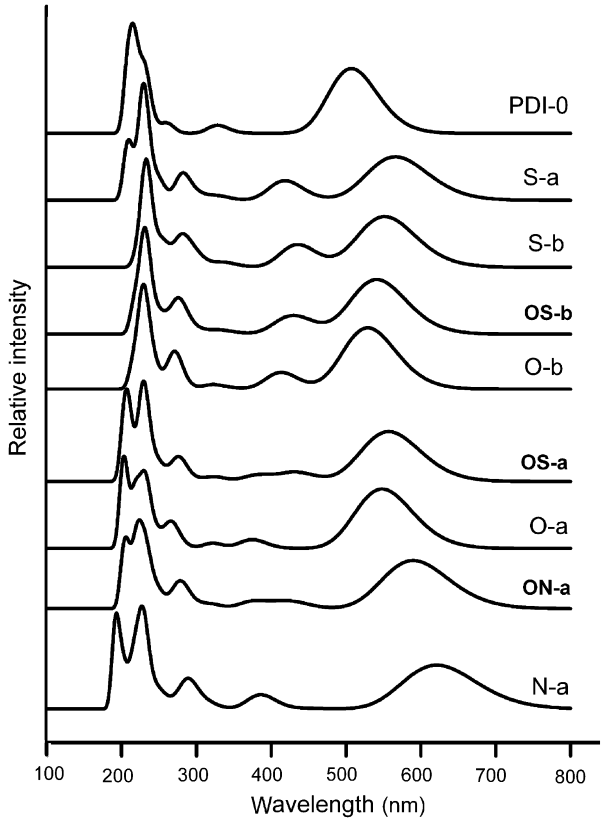

Fig. 4. The simulated electronic absorption spectra of 1,7-disubstituted PDIs.

lowing the order of $CH_3S \rightarrow CH_3O \rightarrow CH_3N$–, while the peaks at 3093 and 3118 cm^{-1} are weakened significantly or even more completely disappeared. The newly appeared peaks at 2952 cm^{-1} for S-a, 2926 cm^{-1} for O-a and 2902 cm^{-1} for N-a are assigned to the symmetric XC–H (X = S, O, N) stretching of the introduced methylthio, methoxy and methylamino groups respectively. The peaks at 2993 and 3044 cm^{-1} in the IR spectra of O-a, which do not shown in the spectra of other compounds, are assigned to the symmetric and asymmetric OC–H stretching vibration of methoxy groups. Same vibration of methylamino groups in N-a appeared at 2979 and 3448 cm^{-1}. Four peaks at 2926, 2952 2993 and 3044 cm^{-1} in the spectra of OS-a, which were not shown by the spectra of PDI-0, were assigned to the OC–H or SC–H stretching vibrations. Six peaks at 2905, 2925, 2990, 2979, 3042 and 3448 cm^{-1} were found in the IR spectra of N-a, which are assigned similarly to the symmetrical or asymmetrical stretching vibration of NC–H of methylamino groups. For compounds S-b, OS-b and O-b, the peaks corresponding to the stretching vibration of C–H on the perylene ring appeared at 2970 and 3028 cm^{-1}. A large new peak near 3088 cm^{-1} was assigned to the C–H stretching vibration of benzene in thiophenyl or phenoxy groups.

The asymmetric and symmetric C=O stretching vibrations of PDI-0 appeared at 1706 and 1674 cm^{-1}, respectively. The introduction of side groups at 1,7 positions of perylene ring do not affect these two vibrations and the peaks keep unchanged in the spectra of other compounds. The peak at 1581 cm^{-1} in the spectrum of PDI-0 corresponds to the wag vibration of C–H on the perylene ring, which are also unaffected by the side groups as revealed by the spectra of other compounds.

In the range of 1570–1450 cm^{-1}, a group of small peaks were found in the spectrum of PDI-0, which are assigned to the in-plane C–H wag and/or C=C stretching of the perylene ring. These peaks were found to be affected by the side groups. The small shoulder at 1567 cm^{-1} in the spectrum of PDI-0 shifts to a lower wave number when side groups are introduced. For example, it is observed at 1547 cm^{-1} for O-a and 1533 cm^{-1} for S-a. The small peaks at 1497 and 1468 cm^{-1} for PDI-0 shifted to 1504 and 1472 cm^{-1} for O-a with obviously increased intensity. The same peaks were shifted to 1493 and 1446 cm^{-1} in the spectrum of S-a and 1485 and 1455 cm^{-1} in the spectrum of N-a. The results suggest that the substitution of side groups at bay positions affect the vibrations of C=C stretching in the perylene ring.

The peaks in the region of 1000–1420 cm^{-1} are assigned to the vibration of deformation of perylene ring and the imide ring. The introduction of side groups brings large changes on both the position and intensity of the peaks in this region. Because the symmetry of the molecule were reduced by the introduction of side groups at 1,7 positions, which brings more vibration models for the molecules, and thus results in more peaks in this region. It is worth noting that the IR spectra of OS-a comprise most of the feather peaks of both O-a and S-a while the IR spectra of ON-a comprise the most feather peaks of N-a and O-a.

3.6. Ionization and affinity

The ionization energy (IE) and electronic affinity (EA) of these compounds were calculated at the B3LYP/6-31G(d) level. The calculated results and experimental data are comparatively summarized in Table 7. The calculated first adiabatic ionization energy

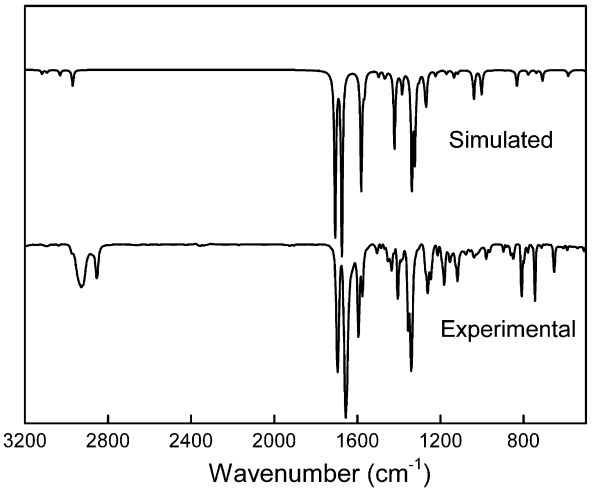

Fig. 5. Comparison between the calculated and experimental IR spectra of PDI-0.

Table 6
The estimated first vertical singlet (S_{1v}) and triplet (T_{1v}) excitation energy of 1,7-disubstituted PDIs (in eV) with TDDFT calculation

Ex. state	PDI-0	S-b	OS-b	O-b	S-a	OS-a	O-a	ON-a	N-a
S_{1v}	2.4448	2.2475	2.2916	2.3434	2.1906	2.2263	2.2621	2.1026	1.9962
T_{1v}	1.2445	1.2863	1.2762	1.2636	1.2181	1.1853	1.1447	1.0824	1.0206

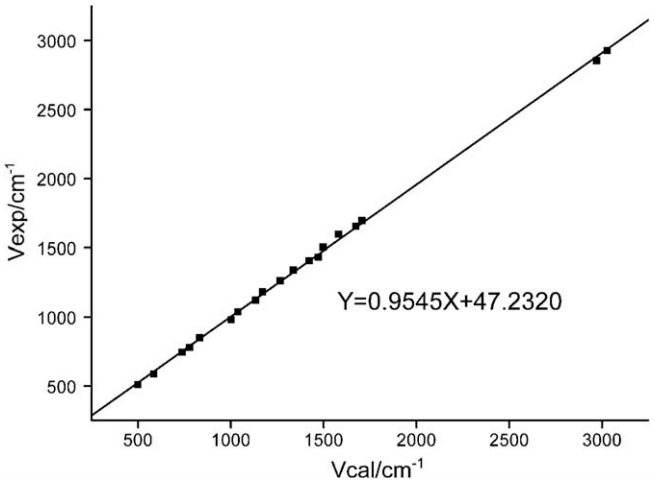

Fig. 6. Consistency of the wavenumbers of the calculated and experimental IR spectra main peaks of PDI-0 (correction coefficient: R = 0.99961 standard deviation: SD = 18.69172).

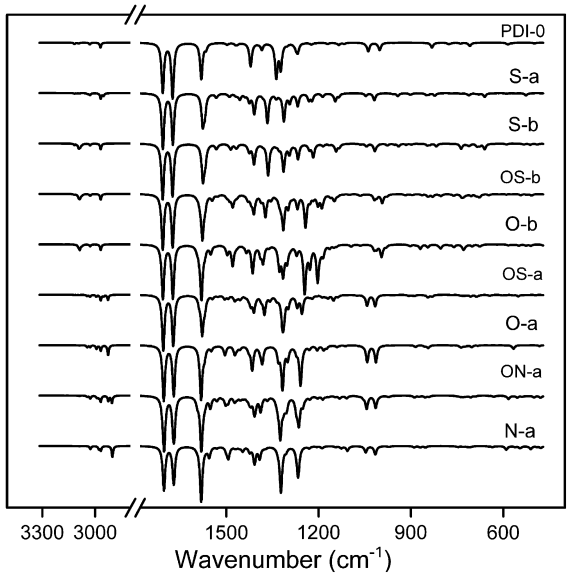

Fig. 7. The normalized and simulated IR spectra of 1,7-substituted PDIs.

of S-a is 6.74 eV, while the vertical ionization energy is 6.88 eV. We use the vertical ionization energy instead of the adiabatic ionization energy in the following discussion. It is necessary to mention that the experimental data are oxidation and reduction potentials relative to normal hydrogen electrode (NHE), while the calculated absolute values are relative to vacuum. Compared to the unsubstituted PDI-0, the ionization energy of the substituted compounds are reduced due to the introduction of the electron donating groups, and agree well with the decrease of the experimental first oxidation potentials. For example, the IE reduced from 7.28 eV for PDI-0 to 6.88, 6.47 and 6.42 eV for S-a, O-a and N-a, respectively, in line with the decrease on first oxidation potentials determined experimentally following the same order. This suggests that the electron donating ability of the side groups decrease following the order of $CH_3NH > CH_3O > CH_3S$. As expected, the IE of OS-a lied between that of S-a and O-a and the IE of ON-a lied between that of N-a and O-a, which agree well with the experimental findings that the first oxidation potential of ON-a, 0.91 eV, lied between 1.31 and 0.72 eV for O-a and N-a, respectively, and that of OS-a, 1.33 eV, lied between 1.37 eV for S-a and 1.31 eV for O-a.

Similarly, the EA of the substituted compounds are depressed due to the electron donating property of the side groups. The EA value increased following the order of S-a < OS-a < O-a < ON-a < N-a, corresponding well with the order of reduction potentials recorded. It is also noted that the calculated EAs for these series compounds corresponds well with the calculated energy levels of LUMOs too.

4. Conclusion

The planar structure of PDI ring is twisted by the substitution at 1,7 positions and the twisting angles were mainly determined by the linking atoms between the side groups and perylene ring due to the steric hindrence. The energy levels calculated based on TDDFT method of HOMO and LUMO and the HOMO–LUMO energy gaps are all reduced by the substitution of electron donating groups at the bay positions. Methylamino groups present larger effects on the HOMO/LUMO energy gap relative to methoxy and methylthio groups because of its strong electron donating abilities. The comparison between the simulated and the experimental absorption spectra of these compounds revealed the different solvation effects of the PDIs with different side groups. The calculated ionization energy (IE) and electronic affinity (EA) of these compounds are well supported by the experimental redox potentials. The electron donating abilities of the side groups, determined almost exclusively by the conjugation of linking atoms with the perylene ring, which decrease following the order of $CH_3NH > CH_3O > CH_3S$. The results of these work revealed that the introducing of side groups at bay positions is an efficient way to modify the physical properties of PDI compounds.

Acknowledgement

Financial support from the Natural Science Foundation of China (Grant No. 20571049, 20771066, 20640420467), Ministry of Education of China, Shandong University, is gratefully acknowledged.

Appendix A. Supplementary data

Supplementary data associated with this article can be found, in the online version, at doi:10.1016/j.molstruc.2008.07.005.

Table 7
The calculated and experimental ionization energy (IE) and electronic affinity (EA) of 1,7-disubstituted PDIs (in eV)

Compounds		PDI-0	S-a	S-b	OS-b	O-b	OS-a	O-a	ON-a	N-a
IE_v	Calcd.	7.28	6.88	6.80	6.81	6.80	6.82	6.74	6.57	6.42
	Exp.[a]	1.62	1.37	1.45	...	1.44	1.33	1.31	0.91	0.72
EA_v	Calcd.	−2.19	−2.11	−2.10	−1.92	−2.06	−2.01	−1.92	−1.88	−1.84
	Exp.[a]	−0.58	−0.62	−0.55	...	−0.85	−0.68	−0.76	−0.78	−0.82

[a] Exp. data taken from [42].

References

[1] J.Z. Sun, Chin. Chem. Lett. 16 (2005) 1201–1204.
[2] C.W. Struijk, A.B. Sieval, J.E.J. Dakhorst, M.V. Dijk, P. Kimkes, R.B.M. Koehrst, H. Donker, T.J. Schaafsma, S.J. Picken, A.M.V.D. Craats, J.M. Warman, H. Zuilhof, E.J.R. Sudhölter, J. Am. Chem. Soc. 122 (2000) 11057–11066.
[3] P.R.L. Malenfant, C.D. Dimitrakopoulos, J.D. Gelorme, L.L. Kosbar, T.O. Graham, A. Curioni, W. Andeoni, Appl. Phys. Lett. 80 (2002) 2517–2519.
[4] M.M. Shi, H.Z. Chen, M. Wang, Acta Chim. Sinica 64 (2006) 721–726.
[5] M. Ling, Z. Bao, P. Erk, M. Koenemann, M. Gomez, Appl. Phys. Lett. 90 (2007) 093508.
[6] S.H. Kim, Y.S. Yang, J.H. Lee, J. Lee, H.Y. Chu, H. Lee, J. Oh, L. Do, T. Zyung, Opt. Mater. 21 (2003) 439–443.
[7] Y. Kim, I. Chung, Y.C. Kim, J. Yu, Chem. Phys. Lett. 398 (2004) 367–371.
[8] Z. An, J. Yu, S.C. Jones, S. Barlow, S. Yoo, B. Domercq, P. Prins, L.D.A. Siebbeles, B. Kippelen, S.R. Marder, Adv. Mater. 17 (2005) 2580–2583.
[9] Z. Chen, M.G. Debije, T. Debaerdemaeker, P. Osswald, F. Würthner, Chem. Phys. Chem. 5 (2004) 137–140.
[10] R.J. Chesterfield, J.C. Mckeen, C.R. Newman, P.C. Ewbank, D.A.D.S. Filho, J. Brédas, L.L. Miller, K.R. Mann, C.D. Frisbie, J. Phys. Chem. B 108 (2004) 19281–19292.
[11] J.H. Schön, C. Kloc, B. Batlogg, Appl. Phys. Lett. 77 (2000) 3776–3778.
[12] C.W. Tang, Appl. Phys. Lett. 48 (1986) 183–185.
[13] A.J. Breeze, A. Salomon, D.S. Ginley, B.A. Gregg, Appl. Phys. Lett. 81 (2002) 3085–3087.
[14] L. Schmidt-Mende, A. Fechtenkötter, K. Müllen, E. Moons, R.H. Friend, J.D. Mackenzie, Science 293 (2001) 1119–1122.
[15] A. Yakimov, S.R. Forrest, Appl. Phys. Lett. 80 (2002) 1667–1669.
[16] L. Tan, M.D. Curtis, A.H. Francis, Chem. Mater. 15 (2003) 2272–2279.
[17] P. Peumans, S. Uchida, S.R. Forrest, Nature 425 (2003) 158–162.
[18] H. Chen, M. Shi, T. Aernouts, M. Wang, G. Borghs, P. Heremans, Sol. Energ. Mat. Sol. C. 87 (2005) 521–527.
[19] Y. Shibano, T. Umeyama, Y. Matano, H. Imahori, Org. Lett. 9 (2007) 1971–1974.
[20] Z. Zhang, Study on Photoelectric Conversion Characteristics of Cuprum Phthalocyanine/ Perylene Diimide Molecular Systems, Doctoral Thesis of Tsinghua University, 2005.
[21] R.S. Loewe, K. Tomizaki, W.J. Youngblood, Z. Bo, J.S. Lindsey, J. Mater. Chem. 12 (2002) 3438–3451.
[22] K. Tomizaki, R.S. Loewe. C. Kirmaier, J.K. Schwartz, J.L. Retsek, D.F. Bocian, D. Holten, J.S. Lindsey, J. Org. Chem. 67 (2002) 6519–6534.
[23] X. Li, L.E. Sinks, B. Rybtchinski, M.R. Wasielewski, J. Am. Chem. Soc. 126 (2004) 10810–10811.
[24] B. Rybtchinski, L.E. Sinks, M.R. Wasielewski, J. Am. Chem. Soc. 126 (2004) 12268–12269.
[25] A.M. Ramos, E.H.A. Beckers, T. Offermans, S.C.J. Meskers, R.A.J. Janssen, J. Phys. Chem. A 108 (2004) 8201–8211.
[26] M.A. Angadi, D. Gosztola, M.R. Wasielewski, Mater. Sci. Eng. B 63 (1999) 191–194.
[27] P. Ranke, I. Bleyl, J. Simmerer, D. Haarer, A. Bacher, H.W. Schmidt, Appl. Phys. Lett. 71 (1997) 1332–1334.
[28] S. Alibert-Fouet, S. Dardel, H. Bock, M. Oukachmih, S. Archambeau, I. Seguy, P. Dntruel, Chem. Phys. Chem. 4 (2003) 983–985.
[29] P. Schouwink, A.H. Schafer, C. Seidel, H. Fuchs, Thin Solid Films 372 (2000) 163–168.
[30] T. Zukawa, S. Naka, H. Okada, H. Onnagawa, J. Appl. Phys. 91 (2002) 1171–1174.
[31] C.-C. You, F. Würthner, J. Am. Chem. Soc. 125 (2003) 9716–9725.
[32] E. Peeters, P.A.V. Hal, C.J. Meskers, R.A.J. Janssen, E.W. Meijer, Chem. Eur. J. 8 (2002) 4470–4474.
[33] R. Dobrawa, F. Würthner, Chem. Commun. (2002) 1878–1879.
[34] M.J. Fuller, L.E. Sinks, B. Rybtchinski, J.M. Giaimo, X. Li, M.R. Wasielewski, J. Phys. Chem. A 109 (2005) 970–975.
[35] S. Xiao, M.E. El-Khouly, Y. Li, Z. Gan, H. Liu, L. Jiang, Y. Araki, O. Ito, D. Zhu, J. Phys. Chem. B 109 (2005) 3658–3667.
[36] A. Sautter, B.K. Kaletas, D.G. Schmid, R. Dobrawa, M. Zimine, G. Jung, I.H.M.V. Stockkum, L.D. Cola, R.M. Wiliams, F. Würthner, J. Am. Chem. Soc. 127 (2005) 6719–6729.
[37] M.P. O'Neil, M.P. Niemczyk, W.A. Svec, D. Gosztola, G.L. Gaines III, M.R. Wasielewski, Science 257 (1992) 63–65.
[38] A.J. Jiménez, F. Spänig, M.S. Rodríguez-Morgade, K. Ohkubo, S. Fukuzumi, D.M. Guldi, T. Torres, Org. Lett. 9 (2007) 2481–2484.
[39] C. You, F. Wurthner, Org. Lett. 6 (2004) 2401–2404.
[40] Y. Chen, Y. Lin, M.E. El-Khouly, X.D. Zhuang, Y.A.O. Ito, W. Zhang, J. Phys. Chem. C 111 (2007) 16096–16099.
[41] M.J. Ahrens, M.J. Tauber, M.R. Wasielewski, J. Org. Chem. 71 (2006) 2107–2114.
[42] C. Zhao, Y. Zhang, R. Li, X. Li, J. Jiang, J. Org. Chem. 72 (2007) 2402–2410.
[43] B. Sun, Y. Zhao, X. Qiu, C. Han, Y. Yu, Z. Shi, Supramol. Chem. (2007) 1–9.
[44] H. Weissman, E. Shirman, T. Ben-Moshe, R. Cohen, G. Leitus, L.J.W. Shimon, B. Rybtchinski, Inorg. Chem. 46 (2007) 4790–4792.
[45] F. Würthner, Chem. Commun. (2004) 1564–1579.
[46] Y. Zhao, M. Wasielewski, Tetrahedron Lett. 40 (1999) 7047–7050.
[47] A.Y. Kobitski, R. Scholz, D.R.T. Zahn, J. Mol. Struct. (Theochem) 625 (2003) 39–46.
[48] A.D. Becke, Phys. Rev. A 38 (1988) 3098–3100.
[49] A.D. Becke, J. Chem. Phys. 98 (1993) 5648–5652.
[50] C. Lee, W. Yang, R.G. Parr, Phys. Rev. A 37 (1988) 785–789.
[51] X. Cai, Y. Zhang, X. Zhang, J. Jiang, J. Mol. Struct. (Theochem) 812 (2007) 63–70.
[52] A.E. Clark, C. Qin, A.D.Q. Li, J. Am. Chem. Soc. 129 (2007) 7586–7595.
[53] M. Andrzejak, M. Sterzel, M.T. Pawlikowski, Spectrachim. Acta A 61 (2005) 2029–2032.
[54] F. Pichierri, J. Mol. Struct. (Theochem) 686 (2004) 57–63.
[55] K.K. Ong, J.O. Jensen, H.F. Hameka, J. Mol. Struct. (Theochem) 459 (1999) 131–144.
[56] M. Preuss, R. Miotto, Phys. Rev. B 74 (2006) 115402.
[57] V. Shklover, F.S. Tautz, R. Scholz, S. Sloboshnin, M. Sokolowski, J.A. Schaefer, E. Umbach, Surface Science 454–456 (2000) 60–66.
[58] A. Aldongarov, N.N. Barashkov, I.S. Irgibaeva, Int. J. Quantum Chem. 107 (2007) 2331–2342.
[59] K. Heimer, J. Wuesten, S. Lach, C. Ziegler, J. Chem. Phys. 126 (2007) 164709.
[60] H. Langhals, W. Jona, Eur. J. Org. Chem. 63 (1998) 847–851.
[61] P.C. Hariharan, J.A. Pople, Mol. Phys. 27 (1974) 209–214.
[62] M.D. Halls, J. Velkovski, H.B. Schlegel, Theor. Chem. Acc. 150 (2001) 413–421.
[63] A.P. Scott, L. Radom, J. Phys. Chem. 100 (1996) 16502–16513.
[64] A.E. Reed, L.A. Curtiss, F. Weinhold, Chem. Rev. 88 (1988) 899–926.
[65] S.I. Gorelsky, SWizard program, Available from: %3chttp://www.sg-chem.net/%3e.
[66] M.J. Frisch, G.W. Trucks, H.B. Schlegel, G.E. Scuseria, M.A. Robb, J.R. Cheeseman, J.A. Montgomery, Jr., T. Vreven, K.N. Kudin, J.C. Burant, J.M. Millam, S.S. Iyengar, J. Tomasi, V. Barone, B. Mennucci, M. Cossi, G. Scalmani, N. Rega, G.A. Petersson, H. Nakatsuji, M. Hada, M. Ehara, K. Toyota, R. Fukuda, J. Hasegawa, M. Ishida, T. Nakajima, Y. Honda, O. Kitao, H. Nakai, M. Klene, X. Li, J.E. Knox, H.P. Hratchian, J.B. Cross, C. Adamo, J. Jaramillo, R. Gomperts, R.E. Stratmann, O. Yazyev, A.J. Austin, R. Cammi, C. Pomelli, J.W. Ochterski, P.Y. Ayala, K. Morokuma, G.A. Voth, P. Salvador, J.J. Dannenberg, V.G. Zakrzewski, S. Dapprich, A.D. Daniels, M.C. Strain, O. Farkas, D.K. Malick, A.D. Rabuck, K. Raghavachari, J.B. Foresman, J.V. Ortiz, Q. Cui, A.G. Baboul, S. Clifford, J. Cioslowski, B.B. Stefanov, G. Liu, A. Liashenko, P. Piskorz, I. Komaromi, R.L. Martin, D.J. Fox, T. Keith, M.A. Al-Laham, C.Y. Peng, A. Nanayakkara, M. Challacombe, P.M.W. Gill, B. Johnson, W. Chen, M.W. Wong, C. Gonzalez, J.A. Pople, Gaussian 03, Revision B.05; Gaussian, Inc.: Pittsburgh, PA, 2003.
[67] W. Su, Y. Zhang, C. Zhao, X. Li, J. Jiang, Chem. Phys. Chem. 8 (2007) 1–7.
[68] E. Clementi, D.L. Rainmondi, W.P. Reinhardt, J. Chem. Phys. 38 (1963) 2686–2689.
[69] E. Hadicke, F. Graser, Acta Crystallogr. C (Cr. Str. Comm.) 42 (1986) 189–195.